CrystEngComm

Improved Quantum Yield in Geometrically Constrained Tetraphenylethylene-Based Metal-Organic Frameworks

Journal:	*CrystEngComm*
Manuscript ID	CE-COM-03-2023-000228.R1
Article Type:	Communication
Date Submitted by the Author:	06-Apr-2023
Complete List of Authors:	Stawiasz, Katherine; University of Illinois Urbana-Champaign Deneff, Jacob; Sandia National Laboratories, Department of Nanoscale Sciences Reyes, Raphael; Sandia National Laboratories, Department of Nanoscale Sciences Woods, Toby; University of Illinois at Urbana-Champaign, School of Chemical Sciences Shea-Rohwer, Lauren; Sandia National Laboratories Valdez, Nichole; Sandia National Laboratories Rodriguez, Mark; Sandia National Laboratories, Lawal, Abdul Afeez; University of Illinois Urbana-Champaign Moore, Jeffrey; University of Illinois at Chicago, Sava Gallis, Dorina; Sandia National Laboratories, Department of Nanoscale Sciences

COMMUNICATION

Improved Quantum Yield in Geometrically Constrained Tetraphenylethylene-Based Metal-Organic Frameworks

Received 00th January 20xx,
Accepted 00th January 20xx

DOI: 10.1039/x0xx00000x

Katherine J. Stawiasz,[a,b] Jacob I. Deneff, [c] Raphael A. Reyes,[c] Toby J. Woods,[f] Lauren E. S. Rohwer,[d] Nichole Valdez,[e] Mark A. Rodriguez,[e] Abdul Lawal,[b] Jeffrey S. Moore,[a,b] and Dorina F. Sava Gallis*[c]

Herein, we report the synthesis of a novel, tetraphenylethylene-based ligand for metal-organic frameworks (MOFs). Incorporation of this ligand into a Zn- or Eu-based MOF increased the quantum yield (QY) by almost 2.5x compared to the linker alone. Furthermore, the choice of guest solvent impacted the QY and solvatochromatic response. These shifts are consistent with solvent dielectric constant as well as molecular polarizability.

The ability to detect small changes in local environment is a valuable property across medicine, industry, and in national security. [1, 2, 3] Thus, the investigation of sensing materials, *i.e.* materials that reliably transform a stimulus into a readable signal, is expansive and diverse. Metal-organic frameworks (MOFs) are high-surface area, porous materials in which metals or metal clusters are connected in a crystalline lattice by organic linkers.[4, 5] The potential for synergistic effects between the metal and linker, as well as the diversity of potential structures, make them a particularly attractive class of materials for tuneable sensors.[6]

MOFs have been reported previously as solvatochromic materials,[7, 8] in which the color of the material is dependent on guest molecules in the MOF's pores. This change in emission is useful to detect gases such as hydrogen sulfide, ammonia, sulfur dioxide, or nitrous oxides.[9] Solvatochromism has also been observed in luminescent MOFs (LMOFs)[10, 11, 12] where it alters both their color and photoluminescent emission spectrum, and shows great promise for applications in sensors, as well as light emitting diodes, solar cells, and lasers.[13] The specific emissions and response to guests depends on the choice of metal, ligand, and crystal structure of the matrix.

Luminescent materials with high quantum yield (QY) are of particular interest for sensors. Such materials effectively absorb and emit photons without considerable loss to the surroundings, enabling the creation of more sensitive and easily readable sensors. The work presented here is focused on the design of MOF linkers that display aggregation-induced emission (AIE) and become luminescent or give increased QY through fluorophore association, for example in concentrated solutions. This increased QY is due to restricted rotations of groups like phenyl rings that would otherwise freely rotate and dissipate energy nonradiatively (Figure 1A).[14] As these molecules become more immobile due to increased concentration or incorporation into a rigid lattice, their QY increases.

To optimize QY in a solvatochromic MOF, we focused on linker-based emissions using a tetraphenylethylene (TPE) linker.[15, 16, 17, 18] Based on previous literature reports using TPE-based ligands,[19, 20, 21, 22, 23, 24, 25] we hypothesized that the incorporation of a novel AIE molecule into a conformationally restricted matrix improves quantum yields.

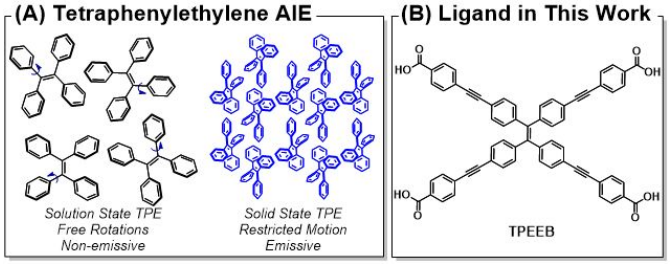

Figure 1. Tetraphenylethylene (TPE) ligands. (A) Differences in TPE between solution state and aggregated state. Note: Torsion angles not drawn to scale. (B) TPE-based ligand used in this work.

[a.] *Beckman Institute for Advanced Science and Technology, University of Illinois at Urbana–Champaign, Urbana, IL 61801, USA.*
[b.] *Department of Chemistry, University of Illinois at Urbana–Champaign, Urbana, IL 61801, USA.*
[c.] *Nanoscale Sciences Department, Sandia National Laboratories, Albuquerque, NM 87185, USA.*
[d.] *Advanced Packaging/Integration Department, Sandia National Laboratories, Albuquerque, NM 87185, USA*
[e.] *Materials Characterization and Performance Department, Sandia National Laboratories, Albuquerque, NM 87185, USA*
[f.] *George L. Clark X-Ray Facility and 3M Materials Laboratory, University of Illinois at Urbana-Champaign, Urbana, IL 61801, USA*
Electronic Supplementary Information (ESI) available: materials, instrumentation, synthetic methods, crystal data, NMR spectra. See DOI: 10.1039/x0xx00000x

Indeed, the matrix coordination-induced emission effect (MCIE) was demonstrated by Dincă and coworkers in 2011 using a TPE-based ligand and Zn metal.[21] The fluorescence quantum yield in that report only increased from 0.8% to 1.8% between the free ligand and MOF; however, upon installation of an alkynyl unit between phenyl rings and a change to meta-substituted carboxylate ligands, they were able to demonstrate fluorescence quantum yields of 9% for the free linker and 35% when the linker was incorporated into a MOF.[19] Notably, the 2012 report focused on ligand design as a means to control the photophysical properties; meta-substitution of the terminal phenyl rings was key to reducing linker fluorescence quenching, both in the free state and in the MOF, compared to the para-substitution employed in previous designs.[26]

To increase the TPE-based MOF's utility as a sensor for a wider variety of molecules, we sought to increase its pore size by expanding the linker while maintaining its intrinsic and desirable photophysical properties. Specifically, we targeted alkynyl extension to preserve rigidity within the linker arms; furthermore, opportunity exists for chemical modification of the alkynyl unit further which could vary properties further. Unlike previous reports with similar molecules,[21] we targeted a para-substituted carboxylic acid. This provided us with a suitable system to study torsion angles in the free linker and the rigidified system, and then compare them with previously published molecules of similar structures.

We utilized the commercially available 1,1,2,2-tetrakis(4-bromophenyl)ethylene to expand the TPE core via metal-mediated cross-coupling. Li and coworkers previously reported using a Suzuki coupling to achieve this, while Dincă and coworkers used Sonogashira couplings to synthesize their linkers.[18] To minimize phenyl ring torsion, we installed an alkynyl linkage with a para-substituted carboxylic ester in 63% yield. After saponification, the resulting molecule, (4,4',4'',4'''-((ethene-1,1,2,2-tetrayltetrakis(benzene-4,1-diyl))tetrakis(ethyne-2,1-diyl))tetrabenzoic acid), was isolated in 93% yield and is colloquially named tetraphenylethylene-ethyne-benzoic acid or **H_4TPEEB** (Figure 1B). For a more detailed description of the synthetic methods used, please refer to the methods section of the SI. We grew X-ray quality crystals from a mixture of dichloromethane and dimethylformamide (Figure 2A). The resulting structure is monoclinic in the space group $P2_1/c$. A data table of crystallographic information for the resolved single crystal is found in Table S1 of the Supporting Information.

We then incorporated the **H_4TPEEB** ligand into MOFs with either transition or rare earth (RE) metal centers to access unique structures directed by the different coordination chemistries, and a broader chemical space to isolate linker effects on luminescence and resulting quantum yield. It was anticipated that the choice of metal and its distinct coordination to the organic ligand would direct distinct MOF structures, contributing to direct alterations in quantum yield.

Accordingly, we accessed two unique structures using either Zn or Eu as the coordinating metal and found that PL linker-based emission properties are dependent on both structural features and guest solvent molecules. Synthesis of a Zn-based framework was accomplished using $Zn(NO_3)_2{\cdot}6H_2O$ as the metal source. Initial attempts in 1:1 dimethylformamide (DMF): ethanol (EtOH) resulted in fine powders which were not suitable for X-ray analysis. To produce better quality crystals, we replaced the DMF solvent with a 1:1 mixture of diethylformamide (DEF): ethanol. Optimizing precursor concentration (see SI Figure S1) led to larger crystals which were suitable for single crystal X-ray diffraction.

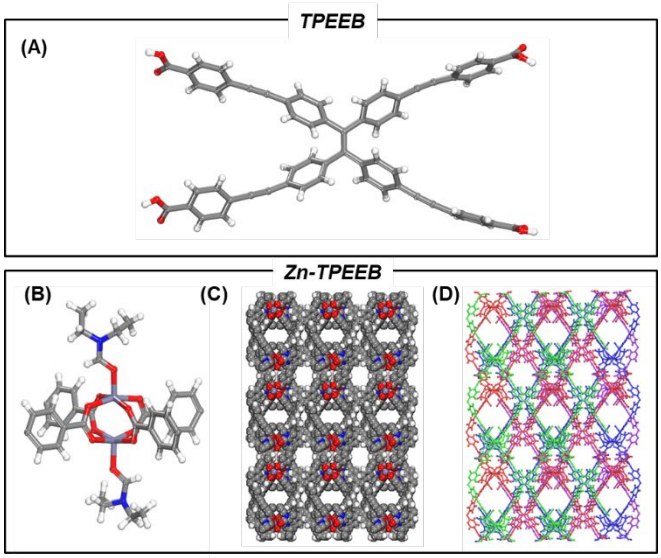

Figure 2. **TPEEB** linker and associated Zn-based MOFs. (A) Structure of **TPEEB** as determined by single crystal X-ray analysis; (B) ball-and-stick representation of Zn paddlewheel; (C) CPK representation of Zn-**TPEEB** (compound 1), displaying open channels along the z axis and (D) ABAB sheet packing highlighted by unique color patterns. Atom color scheme: C= gray, O= red, N= blue, Zn= gray-blue, and H = white. Guest molecules were omitted for clarity.

The resulting crystalline material was characterized and formulated by single crystal X-ray crystallography studies as $[Zn_2(\mathbf{TPEEB})2(DEF)]_{0.5}(DEF)$. The framework is a 2-D coordination polymer (Figure 2B) in which the carboxylate ligand bridges two zinc metal centers to form a paddlewheel complex. The axial sites are occupied by disordered DEF molecules. The resulting sheets stack approximately perpendicularly to the (110) plane. Additional information about the crystal structure can be found in Table S2 of the Supporting Information.

To target the synthesis of an extended 3-D framework based on a metal with 3^+ oxidation state and higher coordination number, the synthesis of an Eu-based **H_4TPEEB** MOF was attempted. [27,28] When $EuCl_3{\cdot}6H_2O$ was reacted with **H_4TPEEB** and 2-flurobenzoic acid in a DMF solution it resulted in crystals with rod-like morphology. As expected, Eu facilitated the formation of a 3-D structures rather than 2-D sheets (Figure 2D-G); however, despite our best efforts to optimize synthetic conditions and crystallographic parameters (*i.e.* long exposure times, varied temperatures, etc.), the low quality of the resulting crystals precluded conclusive statements about the precise bond parameters outside of connectivity (SI, Figure S6).

To probe the host-guest relationship in these systems, the effect of guest solvent within the MOF scaffold on the resulting optical properties was investigated. The Zn-based MOFs were synthesized in DEF/EtOH; the guest molecules in the resulting crystals were subsequently exchanged either with methanol,

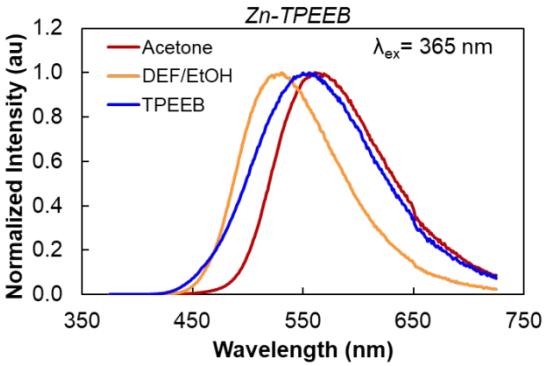

Figure 3. Photoluminescence of the H_4TPEEB linker (blue) and Zn-TPEEB in different solvents.

ethanol, or acetone. The solvent was replenished twice a day for three days. Powder X-ray diffraction (PXRD) studies revealed that acetone best preserved the overall crystallinity of the sample (see SI Figure S4 for more information); this system was therefore chosen for further study.

Photoluminescence emission (PL) and excitation (PLE) measurements were first performed on the **H_4TPEEB** linker alone. In PLE studies, the emission wavelength was 560 nm and the excitation wavelength was scanned between 325 and 550 nm; the peak excitation wavelength was ~365 nm (Figure 3A and 3B). Therefore, samples were excited at 365 nm for both PL and quantum yield (QY) measurements. **H_4TPEEB** was determined to have a QY of 14.0% (Table 1). A lower value for the free linker (Entry 1, Table 1) is in accordance with the accepted hypothesis that molecular motion (*i.e.* torsion, bending, etc.) reduces the observed QY. To determine the effect of rigidification inside a framework, QY was further probed in the Zn-**TPEEB** polymeric sheets. Compared to **H_4TPEEB**, the as-made samples synthesized in DEF/EtOH exhibited a QY of 36.5%.

In addition to the rigidity imparted by the MOF, the guest solvent appeared to play a critical role in the resulting quantum yield. As a general trend, when compared to the free linker, the as-made materials were blue shifted and the solvent exchanged materials were red shifted. While additional solvents were attempted in the solvent exchange study (see SI Figure S4), PXRD showed the broadening and shifting of peaks, inferring significant structural changes. Ultimately, this limited our ability to study a wider range of solvents and their effects on photophysical properties.

The choice of solvent also impacted the observed λ_{max} for PL experiments (Figure 3). When using acetone, the system becomes red-shifted compared to the linker alone; conversely, using DEF or DMF blue shifts the λ_{max}. In 2018, solvatochromatic responses were recorded in rigid, pyrene-based covalent organic frameworks (COFs).[29] It was observed that these solvatochromatic shifts increased monotonically with increasing E_T^N (normalized polarity) of solvent (i.e. Hexanes > EtOH > MeOH > H_2O) for these COF systems.

Surprisingly, a slight deviation from a polarity-based hypothesis for solvatochromatic shift was observed in this work. Notably, as recorded in Table 1, solvent features are described by a variety of metrics. In this case, the data reported here do not follow E_T^N trends (relative polarity) described above, but do align with the solvents dielectric constant (*i.e.,* lower dielectric constants result in higher λ_{max}, smaller molecular polarizability result in higher λ_{max}).

Table 1. Solvent properties including dielectric constants, relative polarity, and molecular polarizability.[30, 31]

Solvent	Relative Polarity (E_T^N)[25]	Dielectric Constant (ε_r)[25]	Molecular Polarizability (Å^3)[26]
Acetone	0.335	20.56	6.47
MeOH	0.762	32.66	3.26
DMF	0.386	36.71	7.93

In addition to solvochromatic changes, significant impact in the QY is noted. For the Zn-based MOFs (Table 2, entries 2-3), QY increased from 36.5% to 40.4% when exchanging the DEF/EtOH guest molecules to acetone. Guest interaction was probed in the Eu-**TPEEB** system using the same methods and observed similar responses to the Zn-**TPEEB** system. The as-made material was found to have a QY of 16.4%, while solvent exchange with methanol increased the QY to 35.3%.

Table 2. Quantum yield measurements. Entries 2 and 3 were synthesized in a 1:1 mixture of diethylformamide: ethanol.

Entry	Compound	Synthesis Solvent	Exchange Solvent	λ_{max} (nm)	QY (%)
1	**H_4TPEEB**	-	-	556	14.0
2	Zn-**TPEEB**	DEF/EtOH	-	531	36.5
3	Zn-**TPEEB**	DEF/EtOH	Acetone	561	40.4

The increased QY observed in the MOF systems is the likely the result of reduced molecular motion within the matrix; the free ligand, being more disordered, has more relaxation pathways that contribute to reduced QY. These results are in accordance with observations made by Wei *et al.* in a similar TPE-based system.[32] In their case, no alkynyl extension is installed between the phenyl units on the arms of the ligand,

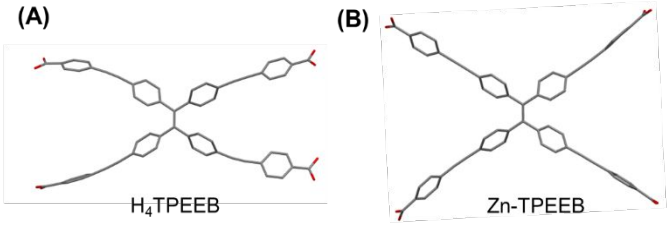

(C)

Compound	Solvent	Planar Angles (°)
H_4TPEEB	DCM/DMF	33.7, 33.9, 74.6, 85.9
Zn-TPEEB	DEF/EtOH	2.4, 11.5, 35.0, 50.3
Zn-TCBPE[a]	DEF/EtOH	18.3, 18.3, 37.5, 37.5
Zn-H_8TDPEPE[b]	DEF/EtOH	10.1, 10.1, 10.1, 10.1

Figure 4. **TPEEB** geometries analysed from single crystal data. (A) Linker structure for free ligand, **H_4TPEEB;** (B) linker in Zn-**TPEEB** MOF; (C) table of phenyl planar angles on each ligand arm.
[a]MOF reported by Li and coworkers.[9]
[b]MOF reported by Dincă and coworkers.[19]

and Zr is used in place of Zn to form a 3-D network. In their system, a 3-fold increase in quantum yield is observed for the MOF network compared to the free linker, similar to the results described herein. One key difference is the QY of Wei's free linker is 30%, giving a MOF-based QY near unity. It is conceivable that with a larger ligand, such as **H_4TPEEB**, more pathways exist for non-radiative decay and a diminished QY is observed.

Furthermore, we quantitatively probed the planar angles of the phenyl rings within arms of the **H_4TPEEB** linker, and the Zn-**TPEEB** sample (Figure 4). The crystal structure obtained from the **H_4TPEEB** linker had planar angles ranging from 33.7-85.9°. Zn-**TPEEB** in DEF exhibited a unique planar angle for each of the four arms: 2.4°, 11.5°, 35.0°, and 50.3° which is quite dissimilar from the four planar angles of 10.1° reported by Dinca.6 Furthermore, Li's TPE-based MOF yielded planar angles of 18.3° and 37.5°.5 Based on the data acquired, there doesn't appear to be a strong correlation between planar angle and quantum yield.

In this work we synthesized the novel TPE-based ligand (4,4',4'',4'''-((ethene-1,1,2,2-tetrayltetrakis(benzene-4,1-diyl))tetrakis(ethyne-2,1-diyl))tetrabenzoic acid), herein called **H_4TPEEB**. Extension of the TPE core was accomplished with a Sonogashira coupling to install alkynyl units between phenyl rings; in addition to an increased pore size, this strategy presents opportunity for post-synthetic modifications (*i.e.* bromination, hydrogenation) to further tune MOF architecture and expand the application space.

It was found that incorporation of **H_4TPEEB** into a metal-organic framework (MOF) could be accomplished using either Zn or Eu metals to form 2-D sheets and 3-D networks, respectively. In quantifying the effect of linker rigidification in these new materials, the resulting quantum yield was increased by roughly 2.5x compared to the linker alone. Furthermore, optical properties of the resulting materials could be modulated based on the chosen guest solvent. This study lays the groundwork for better understanding the correlation between framework characteristics, and ligand geometrical constraints on the resulting optical properties of MOFs; furthermore, it presents a promising new method for the design of stimuli responsive novel materials with increased quantum yield. Efforts are underway to fully utilize these systems as sensing materials.

Author contributions

K.J.S.: conceptualization, methodology, investigation, formal analysis, writing-original draft, writing-review & editing; J.I.D.: methodology, investigation, formal analysis, writing-review & editing; R.A.R. investigation, formal analysis; T.J.W.: resources, formal analysis, investigation, writing-review & editing; L.E.R.: methodology, investigation, formal analysis, writing-review & editing; N.V.: methodology, investigation, formal analysis, writing-review & editing; M.A.R.: methodology, investigation, formal analysis, writing-review & editing; A.L.: investigation, J.S.M.: writing-review & editing, supervision; D.F.S.G.: conceptualization, methodology, investigation, supervision, project administration, funding acquisition, writing-review & editing.

Conflicts of interest

The authors declare no conflicts of interest.

Notes and references

This research was supported by the Laboratory Directed Research and Development Program at Sandia National Laboratories and was performed, in part, at the Center for Integrated Nanotechnologies, an Office of Science User Facility operated for the U.S. Department of Energy (DOE) Office of Science. This article has been authored by an employee of National Technology & Engineering Solutions of Sandia, LLC under Contract No. DE-NA0003525 with the U.S. Department of Energy (DOE). The employee owns all right, title and interest in and to the article and is solely responsible for its contents. The United States Government retains and the publisher, by accepting the article for publication, acknowledges that the United States Government retains a non-exclusive, paid-up, irrevocable, world-wide license to publish or reproduce the published form of this article or allow others to do so, for United States Government purposes. The DOE will provide public access to these results of federally sponsored research in accordance with the DOE Public Access Plan https://www.energy.gov/downloads/doe-public-access-plan. The views expressed in this article do not necessarily represent the views of the U.S. Department of Energy or the United States Government. K.J.S. thanks the Department of Defense for an NDSEG fellowship.

References

1 [1] Haleem, A.; Javaid, M.; Singh, R. P.; Suman, R.; Rab, S. *Sensors International* **2021**, *2*, 100100. https://doi.org/10.1016/j.sintl.2021.100100.

2 [2] Czaja, A. U.; Trukhan, N.; Müller, U. *Chem. Soc. Rev.* **2009**, *38* (5), 1284–1293. https://doi.org/10.1039/B804680H.

3 [3] National Research Council. 2001. *Materials in the New Millennium: Responding to Society's Needs*. Washington, DC: The National Academies Press. https://doi.org/10.17226/10187.

4 [4] Eddaoudi, M.; Kim, J.; Rosi, N.; Vodak, D.; Wachter, J.; O'Keeffe, M.; Yaghi, O. M. *Science* **2002**, *295* (5554), 469–472. https://doi.org/10.1126/science.1067208.

5 [5] Furukawa, H.; Cordova, K. E.; O'Keeffe, M.; Yaghi, O. M. *Science* **2013**, *341* (6149), 1230444. https://doi.org/10.1126/science.1230444.

6 [6] Kumar, P.; Deep, A.; Kim, K.-H. *TrAC Trends in Analytical Chemistry* **2015**, *73*, 39–53. https://doi.org/10.1016/j.trac.2015.04.009.

7 [7] Chen, Q.; Chang, Z.; Song, W.-C.; Song, H.; Song, H.-B.; Hu, T.-L.; Bu, X.-H. *Angewandte Chemie International Edition*

2013, *52* (44), 11550–11553. https://doi.org/10.1002/anie.201306304.

8 [8] Cao, L.-H.; Wei, Y.-S.; Xu, H.; Zang, S.-Q.; Mak, T. C. W. *Advanced Functional Materials* **2015**, *25* (41), 6448–6457. https://doi.org/10.1002/adfm.201503154.

9 [9] Li, H.-Y.; Zhao, S.-N.; Zang, S.-Q.; Li, J. *Chem. Soc. Rev.* **2020**, *49* (17), 6364–6401. https://doi.org/10.1039/C9CS00778D.

10 [10] Cui, Y.; Yue, Y.; Qian, G.; Chen, B. *Chem. Rev.* **2012**, *112* (2), 1126–1162. https://doi.org/10.1021/cr200101d.

11 [11] Lustig, W. P.; Shen, Z.; Teat, S. J.; Javed, N.; Velasco, E.; O'Carroll, D. M.; Li, J. *Chem. Sci.* **2020**, *11* (7), 1814–1824. https://doi.org/10.1039/C9SC05721H.

12 [12] Pan, M.; Liao, W.-M.; Yin, S.-Y.; Sun, S.-S.; Su, C.-Y. *Chem. Rev.* **2018**, *118* (18), 8889–8935. https://doi.org/10.1021/acs.chemrev.8b00222.

13 [13] Zhang, D.; Gu, L.; Zhang, Q.; Lin, Y.; Lien, D.-H.; Kam, M.; Poddar, S.; Garnett, E. C.; Javey, A.; Fan, Z. *Nano Lett.* **2019**, *19* (5), 2850–2857. https://doi.org/10.1021/acs.nanolett.8b04887.

14 [14] Mei, J.; Leung, N. L. C.; Kwok, R. T. K.; Lam, J. W. Y.; Tang, B. Z. *Chem. Rev.* **2015**, *115* (21), 11718–11940. https://doi.org/10.1021/acs.chemrev.5b00263.

15 [15] Andreo, J.; Priola, E.; Alberto, G.; Benzi, P.; Marabello, D.; Proserpio, D. M.; Lamberti, C.; Diana, E. *J. Am. Chem. Soc.* **2018**, *140* (43), 14144–14149. https://doi.org/10.1021/jacs.8b07113.

16 [16] Lu, J.; Xin, X.-H.; Lin, Y.-J.; Wang, S.-H.; Xu, J.-G.; Zheng, F.-K.; Guo, G.-C. *Dalton Transactions* **2019**, *48* (5), 1722–1731. https://doi.org/10.1039/C8DT04587A.

17 [17] Kloepper, R. M.; Wiedenbeck, M. L. *Review of Scientific Instruments* **1952**, *23* (8), 446–447. https://doi.org/10.1063/1.1746358.

18 [18] Yao, H.; Zhou, M.; Yu, X.; Bai, M. *Chem. Commun*. **2022**, *58* (32), 4985–4988. https://doi.org/10.1039/D2CC00722C.

19 [19] Shustova, N. B.; Cozzolino, A. F.; Dincă, M. *J. Am. Chem. Soc.* **2012**, *134* (48), 19596–19599. https://doi.org/10.1021/ja3103154.

20 [20] Lustig, W. P.; Shen, Z.; Teat, S. J.; Javed, N.; Velasco, E.; O'Carroll, D. M.; Li, J. *Chem. Sci.* **2020**, *11* (7), 1814–1824. https://doi.org/10.1039/C9SC05721H.

21 [21] Shustova, N. B.; McCarthy, B. D.; Dincă, M. *J. Am. Chem. Soc.* **2011**, *133* (50), 20126–20129. https://doi.org/10.1021/ja209327q.

22 [22] Yang, L.; Dou, Y.; Qin, L.; Chen, L.; Xu, M.; Kong, C.; Zhang, D.; Zhou, Z.; Wang, S. *Inorg. Chem.* **2020**, *59* (22), 16644–16653. https://doi.org/10.1021/acs.inorgchem.0c02604.

23 [23] Shang, W.; Zhu, X.; Liang, T.; Du, C.; Hu, L.; Li, T.; Liu, M. *Angewandte Chemie International Edition* **2020**, *59* (31), 12811–12816. https://doi.org/10.1002/anie.202005703.

24 [24] Guo, X.; Zhu, N.; Wang, S.-P.; Li, G.; Bai, F.-Q.; Li, Y.; Han, Y.; Zou, B.; Chen, X.-B.; Shi, Z.; Feng, S. *Angewandte Chemie International Edition* **2020**, *59* (44), 19716–19721. https://doi.org/10.1002/anie.202010326.

25 [25] Zhu, Z.-H.; Bi, C.; Zou, H.-H.; Feng, G.; Xu, S.; Tang, B. Z. *Advanced Science* **2022**, *9* (16), 2200850. https://doi.org/10.1002/advs.202200850.

26 [26] Gould, S. L.; Tranchemontagne, D.; Yaghi, O. M.; Garcia-Garibay, M. A. *J. Am. Chem. Soc.* **2008**, *130* (11), 3246–3247. https://doi.org/10.1021/ja077122c.

27 [27] Deneff, J. I.; Butler, K. S.; Rohwer, L. E. S.; Pearce, C. J.; Valdez, N. R.; Rodriguez, M. A.; Luk, T. S.; Sava Gallis, D. F. *Angewandte Chemie* **2021**, *133* (3), 1223–1231. https://doi.org/10.1002/ange.202013012.

28 [28] Deneff, J. I.; Rohwer, L. E. S.; Butler, K. S.; Valdez, N. R.; Rodriguez, M. A.; Luk, T. S.; Sava Gallis, D. F. *ACS Appl. Mater. Interfaces* **2022**, *14* (2), 3038–3047. https://doi.org/10.1021/acsami.1c20432.

29 [29] Ascherl, L.; Evans, E. W.; Hennemann, M.; Di Nuzzo, D.; Hufnagel, A. G.; Beetz, M.; Friend, R. H.; Clark, T.; Bein, T.; Auras, F. Solvatochromic Covalent Organic Frameworks. *Nat Commun* **2018**, *9* (1), 3802. https://doi.org/10.1038/s41467-018-06161-w.

30 [30] Christian Reichardt, *Solvents and Solvent Effects in Organic Chemistry*, Wiley-VCH Publishers, 3rd ed., **2003**.

31 [31] Bosque, R.; Sales, J. Polarizabilities of Solvents from the Chemical Composition. *J. Chem. Inf. Comput. Sci.* **2002**, *42* (5), 1154–1163. https://doi.org/10.1021/ci025528x.

32 [32] Wei, Z.; Gu, Z.-Y.; Arvapally, R. K.; Chen, Y.-P.; McDougald, R. N. Jr.; Ivy, J. F.; Yakovenko, A. A.; Feng, D.; Omary, M. A.; Zhou, H.-C. *J. Am. Chem. Soc.* **2014**, *136* (23), 8269–8276. https://doi.org/10.1021/ja5006866.